ELSEVIER

Bone Vol. 26, No. 6
June 2000:635–642

Low-Megahertz Ultrasonic Properties of Bovine Cancellous Bone

B. K. HOFFMEISTER,[1] S. A. WHITTEN,[1] and J. Y. RHO[2]

[1]*Department of Physics, Rhodes College, Memphis, TN, USA*
[2]*Department of Biomedical Engineering, University of Memphis, Memphis, TN, USA*

Ultrasound offers a noninvasive means to detect changes that occur to the density of cancellous bone as a result of degenerative diseases such as osteoporosis. Techniques based on the velocity and frequency dependence of attenuation of ultrasonic pulses propagated through cancellous bone have proven sensitive to bone density. Most previous studies have investigated these two parameters in the frequency range of 0.1–1.0 MHz. The present study had two goals. The first was to measure three ultrasonic parameters: longitudinal mode velocity; broadband ultrasonic attenuation (BUA); and apparent integrated backscatter (AIB), at higher frequencies using a broadband 2.25 MHz measurement system. The second goal was to assess the dependence of these parameters on bone density. Twenty-one specimens of cancellous bone acquired from the proximal end of four bovine tibiae were investigated in this study. The apparent density of the specimens (determined with the bone marrow removed and the specimens thoroughly dry) ranged between 0.3 and 0.9 g/cm^3. Ultrasonic measurements were performed along three mutually perpendicular directions corresponding to the anteroposterior (AP), mediolateral (ML), and superoinferior (SI) axes of the tibia. A linear regression was used to analyze the results of these measurements as a function of apparent density. Velocity demonstrated a highly significant linear increase with density for all three directions (AP: $p < 0.001$; ML: $p < 0.001$; SI: $p < 0.01$). AIB decreased with density in all three directions; however, only the ML and SI directions demonstrated a significant linear correlation (AP: p = n.s.; ML: $p < 0.05$; SI: $p < 0.05$). In the frequency range 0.5–1.0 MHz, BUA exhibited a significant linear increase in the AP and ML directions, but not the SI direction (AP: $p < 0.05$; ML: $p < 0.01$; SI: p = n.s.). In contrast, in the frequency range 1.0–2.0 MHz, BUA exhibited a highly significant increase with density in the SI direction, but no significant change in the AP and ML directions (AP: p = n.s., ML: p = n.s., SI: $p < 0.001$). (Bone 26:635–642; 2000)

Key Words: Cancellous bone; Ultrasound; Backscatter; Attenuation; Velocity; Density.

Address for correspondence and reprints: Dr. Brent K. Hoffmeister, Rhodes College Department of Physics, Memphis, TN 38112. E-mail: hoffmeister@rhodes.edu

Introduction

In recent years, a number of studies have been conducted to assess the ultrasonic properties of cancellous and cortical bone. The two most thoroughly investigated properties have been ultrasonic velocity and attenuation.[6,7,12,15,20] These parameters have demonstrated a sensitivity to bone mineral density (BMD), an important predictor of fracture risk in degenerative diseases such as osteoporosis. Clinical systems based on these ultrasonic parameters typically operate at center frequencies near 0.5 MHz.

Ultrasound is also widely used for imaging soft tissues in the human body. Ultrasonic imaging systems operate by transmitting broadband ultrasonic pulses in a two-dimensional plane and processing the received backscattered signals to produce cross-sectional images of the interrogated region. In a recent study, Wear and Garra used such an imaging system to assess BMD in healthy human volunteers.[24] The system they used was operated at a center frequency of 2.25 MHz, a common choice for imaging soft tissues in adult human subjects. Their study suggested that parameters based on ultrasonic backscatter may be sensitive to bone density.

Techniques based on ultrasonic backscatter offer the advantage that only one ultrasonic transducer is required to perform measurements because the same transducer acts as a transmitter and receiver of acoustic energy. For clinical bone assessment, this feature would dramatically increase the number of sites in the body accessible to ultrasonic interrogation. In contrast, most clinically applicable techniques of measuring velocity and attenuation require two transducers to be placed on either side of the bone with one acting as a transmitter and the other as a receiver. This significantly limits the number of locations in the body accessible to ultrasonic study, and is one of the reasons the calcaneus is a site favored by many investigators.

Ultrasonic scattering occurs when an ultrasonic wave encounters inhomogeneities that possess a different acoustic impedance than the surrounding medium. Tissue characterization techniques based on ultrasonic backscatter have been shown to be sensitive to the inhomogeneous and anisotropic nature of a variety of soft tissues.[1–5,8,10,11,13,25] It is hypothesized that changes in BMD affect the degree of inhomogeneity of cancellous bone, and that ultrasonic backscatter may be sensitive to these changes.

Most recent ultrasonic studies of cancellous bone have been conducted at frequencies of <1 MHz. Consequently, little is known about the ultrasonic properties of cancellous bone at higher frequencies comparable to those used for diagnostic imaging. The goal of this study was to investigate the dependence of parameters related to ultrasonic velocity, attenuation, and backscatter on bone density using a broadband ultrasonic

8756-3282/00/$20.00
PII S8756-3282(00)00275-1

Bone Vol. 26, No. 6
June 2000:635–642

measurement system operating at a center frequency of 2.25 MHz.

Materials and Methods

Samples of cancellous bone used for this study were obtained from four fresh frozen bovine tibiae. Samples were prepared from the proximal end of the bone using a band saw to make three transverse cuts oriented parallel to the articular surface. These sections were subdivided into approximately cubic specimens with a side length of roughly 20 mm. The surfaces of each specimen were finished with a slow-speed diamond wafering saw. The resulting specimens had flat and parallel faces with side lengths ranging between 12 and 18 mm. To facilitate easier handling and storage of the specimens, a water jet was used to remove most of the bone marrow. A permanent marker was used to place a fiducial mark on the specimens to record their orientation relative to the anteroposterior (AP), mediolateral (ML), and superoinferior (SI) axes of the tibia. A total of 21 specimens were prepared in this fashion. Care was taken to remove air bubbles before ultrasonic measurements by degassing the specimens under vacuum. The specimens were stored in a refrigerated saline solution.

To measure mass density, the specimens were allowed to thoroughly air dry at room temperature for 3 days, after which their masses were measured. Volume was determined by measuring the exterior dimensions of the cubes with calipers. Apparent density was determined by dividing the mass of each specimen by its volume. The word "apparent" indicates that density was determined with the bones in a dry condition and most of the bone marrow removed. Thus, apparent density represents the density of the porous specimen, and not the density of the trabeculae.

Ultrasonic measurements were made in a water bath maintained at room temperature. The temperature of the water ranged between 20.8°C and 25.5°C with a maximum change of less than 1°C for any single specimen. A pair of transducers (Panametrics V306, 2.25 MHz, 0.5 in. diameter) were oriented vertically facing each other. The faces of the transducers were separated by 8 cm, a distance slightly greater than the 6 cm near-field distance stated by the manufacturer. The vertical orientation of the transducers made it possible to rest the specimens directly on the face of the receiving transducer. This simplified the positioning and support of the specimens. The transducers were connected to an ultrasonic pulser-receiver (Panametrics 5800) that could be operated in a through-transmission or pulse-echo mode. Signals were acquired using a 150 MHz digitizing oscilloscope (Hewlett Packard 54602B) and transferred via a GPIB interface to a personal computer (Power Macintosh 7600/132). Interface and analysis software were designed using LabView. A block diagram of the measurement system is illustrated in **Figure 1**.

Longitudinal mode ultrasonic velocity was determined with the measurement system operating in a through-transmission mode. Data were acquired according to the following procedure. First, a reference signal was obtained by propagating an ultrasonic pulse from the transmitting transducer to the receiving transducer with the sample removed. The sample was then placed between the transducers as illustrated in Figure 1. This reduced the time of flight of the ultrasonic pulse between the transducers because the speed of sound through the sample was greater than water. The difference in these times was denoted by the positive quantity:

$$\Delta t = t_{\text{reference}} - t_{\text{sample}} \tag{1}$$

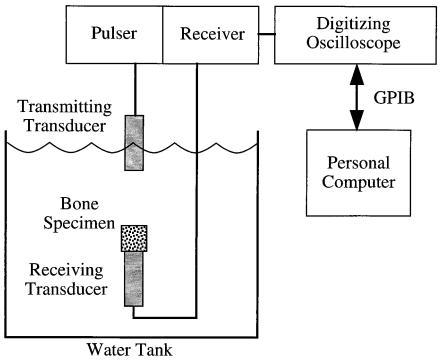

Figure 1. Block diagram of the ultrasonic measurement system used in this study.

For each direction of propagation, the digitized reference signal and sample signal were loaded into a program that allowed the user to place cursors manually on the signals to determine the time of flight of each pulse. The cursors were positioned at times when the received pulse first deviated from the baseline. The velocity of the pulse through the sample was calculated using the equation:

$$c_{\text{sample}} = c_{\text{water}}/(1 - c_{\text{water}}\Delta t/l) \tag{2}$$

where l represents the thickness of the sample. The speed of sound through water, c_{water}, was calculated as a function of temperature T (in °C) according to the fifth-order polynomial expression known as Slutsky's formulation[19]:

$$\begin{aligned} c_{\text{water}} = {} & 1402.73 + 5.03358 \times T \\ & - 5.79506 \times 10^{-2} \times T^2 \\ & + 3.31636 \times 10^{-4} \times T^3 \\ & - 1.45262 \times 10^{-6} \times T^4 \\ & + 3.0449 \times 10^{-9} \times T^5 \end{aligned} \tag{3}$$

The procedure was repeated with each face of the sample oriented to be the incident face. The two measurements obtained for each direction (AP, ML, SI) were averaged to obtain a single value for velocity in that direction.

Broadband ultrasonic attenuation (BUA) was analyzed using the same signals acquired for our velocity measurements. BUA was calculated for each sample, and each direction of propagation, in the following steps. A 15 μs rectangular window was applied to the appropriate reference signal with the ultrasonic pulse approximately centered in the window. A fast Fourier transform (FFT) was used to obtain the power spectrum of the reference signal (in decibels). Next, the process was repeated to obtain the power spectrum of an ultrasonic pulse propagated through the sample. The sample power spectrum was subtracted from the reference power spectrum to obtain signal loss as a function of frequency. A linear fit was performed over the bandwidth of interest, and the slope of the fitted line was divided by the thickness of the sample to obtain a value of BUA in units of decibels per centimeter per megahertz. It should be noted that this approach differs from clinical systems that report BUA in units of decibels per megahertz. Such systems do not normalize for sample thickness as we chose to do for this study. The procedure was repeated with each face of the sample oriented to be the incident face. The two measurements obtained for each

direction (AP, ML, SI) were averaged to obtain a single value for BUA in that direction.

Apparent integrated backscatter (AIB) measurements were obtained by operating the measurement system in a pulse-echo mode. In this mode, the transmitting transducer also served as the receiving transducer. Reference signals were acquired by reflecting ultrasonic pulses off the surface of a 12.7-mm-thick glass optical flat. The reflector was placed directly on the face of the receiving transducer (which was disconnected for these measurements), and was aligned by maximizing the amplitude of the reflected signal. Signals from bone were acquired by replacing the reflector with the sample of interest.

AIB was determined in the following manner. A reference power spectrum was obtained by centering a 4 μs rectangular window on the reflected ultrasonic pulse, and performing an FFT. The power spectrum of the signal backscattered from the sample was obtained through a similar procedure except that the window was positioned 2 μs after the first arrival of acoustic energy from the sample. This was done to exclude the large specular echo produced by the abrupt change in acoustic impedance at the interface between the sample and the water bath. The reference spectrum was subtracted from the sample spectrum, and the result was averaged (integrated) over the bandwidth 1–3 MHz to obtain a single averaged value for backscatter in decibels. We refer to these backscatter values as "apparent" because no compensation is made for the effects of attenuation.

The procedure was repeated with each face of the sample oriented to be the incident face. Five measurements were obtained from each face by laterally translating the sample to locate the ultrasonic beam at five spatially independent sites on the sample. Thus, a total of ten measurements were made on each sample for each direction of propagation (AP, ML, SI). These ten measurements were averaged to obtain a single spatially averaged value for AIB for each direction.

Additional procedures were performed to ensure that the measurement system could operate sensitively over the range of frequencies selected for this study. To assess the reproducibility of our measurements, a single specimen was measured four times according to the following procedure. The sample in saline solution was removed from refrigeration and degassed under vacuum to remove air bubbles. The sample was placed in the water tank used for ultrasonic measurements, and allowed to reach thermal equilibrium with the surrounding water. AIB, BUA, and velocity were measured along the ML direction according to the procedures already described. The sample was then replaced in the saline solution for 1 h, after which the measurements were repeated in a second trial. Three days later, two more trials were performed on the same sample in the same way for a total of four trials of each measurement. The mean and standard deviation of the ultrasonic measurements are reported in **Table 1**. The coefficient of variation for each measurement was determined by dividing the standard deviation by the mean. It should be noted that the sample was positioned manually in each trial, and the position of the ultrasonic beam on the sample could not be exactly duplicated between measurements. This may account for some of the variation in our measurements.

To assess the signal-to-noise ratio of the measurement system, data from a specimen with an intermediate density (0.587 g/cm^3) were analyzed according to the following procedure. Signal power was determined by centering a window on the signal of interest and performing an FFT to determine the signal power spectrum in decibels. The window durations duplicated those used for the analysis of AIB and BUA (4 and 15 μs, respectively). The window was then repositioned on a portion of the acquired trace immediately preceding the arrival of the ultrasonic signal. An FFT was performed to determine the noise power spectrum in decibels. The signal-to-noise ratio was analyzed by subtracting the noise spectrum from the signal spectrum, and frequency averaging the result over bandwidths corresponding to those that were used for the analysis of AIB and BUA. **Table 2** summarizes the results of this analysis.

Table 1. Results of a procedure that was performed to assess the reproducibility of the measurements reported in this study

Measurement	Mean	Standard deviation	Coefficient of variation
Velocity (m/sec)	2284	83	3.6%
BUA (dB/cm · MHz) 0.5–1.0 MHz	56.39	2.83	5.0%
BUA (dB/cm · MHz) 1.0–2.0 MHz	12.03	0.70	5.8%
AIB (dB)	−34.91	0.65	1.9%

Four trials of each measurement were performed along the mediolateral direction of the same specimen. After each trial, the specimen was completely removed from the measurement system and then replaced for the next trial. The coefficient of variation represents the ratio of the standard deviation to the mean.
KEY: AIB, apparent integrated backscatter; BUA, broadband ultrasonic attenuation.

Results

Figure 2 illustrates the results we obtained for longitudinal mode ultrasonic velocity as a function of apparent density. Separate linear regressions were performed for each direction of propagation. Velocity demonstrated a highly significant linear increase with apparent density for all three directions (AP: $p < 0.001$; ML: $p < 0.001$; SI: $p < 0.01$). The elevated values for the SI direction indicate an anisotropy in these specimens. **Table 3** reports mean values of velocity and the corresponding standard deviations for each direction of propagation.

Figures 3 and **4** illustrate the results we obtained for BUA as a function of apparent density using a bandwidth of 0.5–1.0 MHz and 1.0–2.0 MHz, respectively. Little useful acoustic energy was received in a through-transmission mode for frequencies >2.0 MHz. Linear regressions performed on the data illustrated in Figure 3 revealed that, in the frequency range of 0.5–1.0 MHz, BUA exhibited a significant linear increase with increasing density in the AP and ML directions, but not the SI direction (AP: $p < 0.05$; ML: $p < 0.01$; SI: $p =$ n.s.). In contrast, in the frequency range of 1.0–2.0 MHz, only the SI direction exhibited a significant dependence on density as illustrated in Figure 4 (AP: $p =$ n.s.; ML: $p =$ n.s.; SI: $p < 0.001$). For both bandwidths the SI direction was notably different from the AP and ML directions, indicating an anisotropy in this parameter. Table 3

Table 2. Summary of an analysis that was performed to determine the signal to noise ratio of the measurement system

Signal type	Bandwidth (MHz)	Signal-to-noise ratio (dB)
Pulse transmitted through water only	0.5–1.0	16.2
Pulse transmitted through water only	1.0–2.0	33.1
Pulse reflected from glass flat	1.0–3.0	37.9
Pulse transmitted through sample	0.5–1.0	21.1
Pulse transmitted through sample	1.0–2.0	11.1
Backscattered signal from sample	1.0–3.0	30.2

The analysis considered four different types of signals acquired in this study and the different bandwidths over which the signals were analyzed.

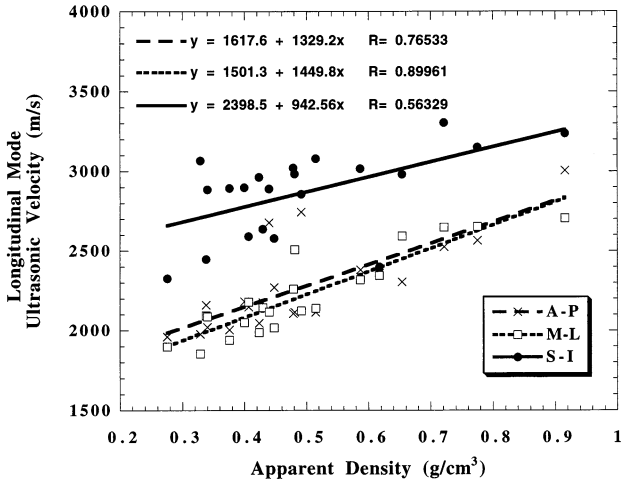

Figure 2. Longitudinal mode ultrasonic velocity plotted as a function of apparent bone density. A linear regression was performed on the data to obtain the reported correlation coefficients for each direction of propagation (anteroposterior, mediolateral, superoinferior).

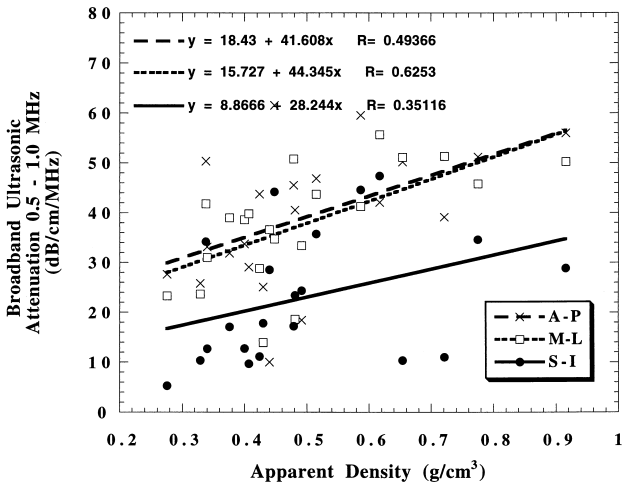

Figure 3. Broadband ultrasonic attenuation (BUA) plotted as a function of apparent bone density. Data were analyzed over the bandwidth 0.5–1.0 MHz. A linear regression was performed on the data to obtain the reported correlation coefficients for each direction of propagation (anteroposterior, mediolateral, superoinferior).

reports mean values for BUA and the corresponding standard deviations for each direction of propagation.

Figure 5 illustrates the results we obtained for AIB as a function of apparent density using a bandwidth of 1.0–3.0 MHz. AIB exhibited a significant linear decrease with increasing bone density in the ML and SI directions (AP: p = n.s.; ML: $p < 0.05$; SI: $p < 0.05$). It is of interest to note that the density dependence of backscatter is approximately the same for all three directions, suggesting that AIB is not as sensitive to the anisotropic nature of cancellous bone as velocity and BUA. This is somewhat surprising, given the fact that this parameter has demonstrated a pronounced anisotropy in tendon and other soft tissues.[8,13,25] Table 3 reports mean values for AIB and the corresponding standard deviations for each direction of propagation.

Discussion

As reported recently by Hosokawa and Otani, longitudinal mode ultrasonic waves propagate as both slow and fast waves in cancellous bone.[9] This phenomenon is characteristic of acoustic wave propagation in a fluid-saturated porous solid. As illustrated in **Figure 6**, we observed evidence of a similar effect in which the broadband ultrasonic pulses we used appeared to separate into a low-frequency fast wave and a high-frequency slow wave. This effect generally was observed to be most pronounced for propagation in the SI direction. To determine velocity, our analysis used the time of first arrival of acoustic energy. Therefore, our velocity measurements specifically refer to the velocity of fast waves through cancellous bone.

Previous studies have shown that ultrasonic velocity depends on the density of cancellous bone and the direction of propagation of the ultrasonic wave.[6,9,15,17,22,23] Our results agree well with these findings. As illustrated in Figure 2, we observed a density dependence of velocity for all three orthogonal directions (AP, ML, SI) under consideration in this study. In addition, our specimens of cancellous bone demonstrated a substantial anisotropy, with maximum velocity occurring for wave propagation along the SI direction.

For this study we measured BUA over two bandwidths: 0.5–1.0 MHz and 1.0–2.0 MHz. Care was taken to ensure that the measurement system could operate sensitively over this range of frequencies. The frequency response of the measurement system is illustrated in **Figure 7**. This power spectrum was obtained from a reference signal with the measurement system operated in a through-transmission mode, and with the sample removed. It is typical of all reference spectra obtained in this study. The bandwidth of the measurement system is determined primarily by the transducer. The spectrum shows that the center frequency of the response is very near the 2.25 MHz value quoted by the manufacturer. The 20 dB bandwidth of the system is approximately 0.5–3.5 MHz.

The power spectrum changes dramatically when the ultrasonic pulse is propagated through a specimen. **Figure 8** illustrates typical power spectra that are obtained when an ultrasonic pulse is propagated along the three different directions considered in this study. As a result of increased attenuation at higher frequencies, the center frequency of all three spectra are shifted

Table 3. Results for longitudinal mode ultrasonic velocity, broadband ultrasonic attenuation (BUA), and apparent integrated backscatter (AIB) averaged along the anteroposterior (AP), mediolateral (ML), and superoinferior (SI) directions for all 21 specimens investigated in this study (mean ± SD)

Direction	Longitudinal mode ultrasonic velocity (m/sec)	BUA 0.5–1.0 MHz (dB/cm · MHz)	BUA 1.0–2.0 MHz (dB/cm · MHz)	AIB (dB)
AP	2279 ± 282	39.13 ± 13.67	8.76 ± 5.48	−34.26 ± 2.39
ML	2222 ± 261	37.78 ± 11.50	12.23 ± 5.87	−33.93 ± 2.13
SI	2867 ± 271	22.91 ± 13.04	7.38 ± 6.07	−34.55 ± 2.78

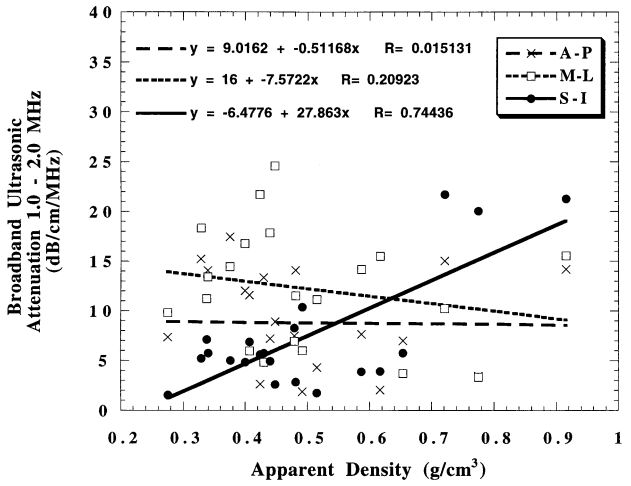

Figure 4. Broadband ultrasonic attenuation (BUA) plotted as a function of apparent bone density. Data were analyzed over the bandwidth 1.0–2.0 MHz. A linear regression was performed on the data to obtain the reported correlation coefficients for each direction of propagation (anteroposterior, mediolateral, superoinferior).

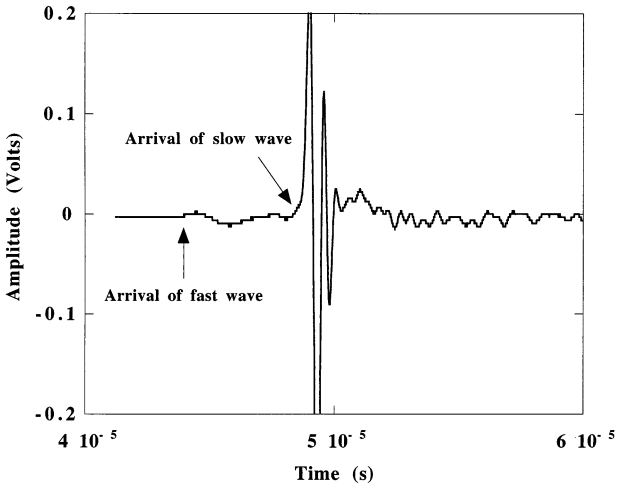

Figure 6. A time-domain signal obtained by propagating an ultrasonic pulse through a specimen of cancellous bone. The pulse appears to separate into two components representing a fast wave and slow wave as indicated. The time of arrival of the fast wave was used to determine velocity.

toward lower frequencies. The bandwidths, however, vary widely. Based on these observations we chose not to restrict ourselves to a single bandwidth for analysis. Rather, we chose two bandwidths: 0.5–1 MHz and 1–2 MHz.

One rationale for these two specific choices of bandwidth was an interesting behavior in the frequency dependence of attenuation around 1 MHz. As illustrated in **Figure 9**, the frequency dependence of attenuation is approximately linear between 0.5 and 1 MHz and 1 and 2 MHz. The slope, however, is not the same for these two bandwidths, changing rather sharply at 1 MHz. This feature was noted in approximately half the samples investigated, and was most prominent for waves propagated along the SI direction. A similar feature was noted by Langton *et al*. in a study utilizing a bandwidth of 100 kHz to 1 MHz in which they noted a sudden decrease in slope at around 600 kHz in healthy human subjects.[12]

A number of studies have been conducted to assess the density dependence of BUA in cancellous bone. It would be useful to compare the results of the present study to those previous studies. This proves difficult for two reasons. First, very few studies have been conducted at frequencies of >1 MHz. Our results suggest that the frequency dependence of attenuation in bovine cancellous bone may change at higher frequencies with a transition in the slope occurring around 1 MHz. Second, most recent studies have investigated human bone. Human cancellous bone typically spans a lower range of apparent densities (0.1–0.4 g/cm^3) than bovine cancellous bone (0.3–0.9 g/cm^3). As demonstrated by Serpe and Rho, BUA may not increase linearly with density over the entire density range of 0.0–1.0 g/cm^3.[18] Therefore, it is not valid to assume that specimens of bovine cancellous

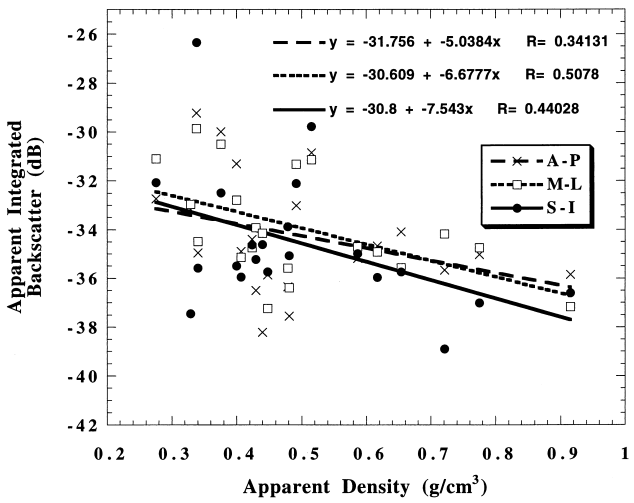

Figure 5. Apparent integrated backscatter (AIB) plotted as a function of apparent bone density. A linear regression was performed on the data to obtain the reported correlation coefficients for each direction of propagation (anteroposterior, mediolateral, superoinferior).

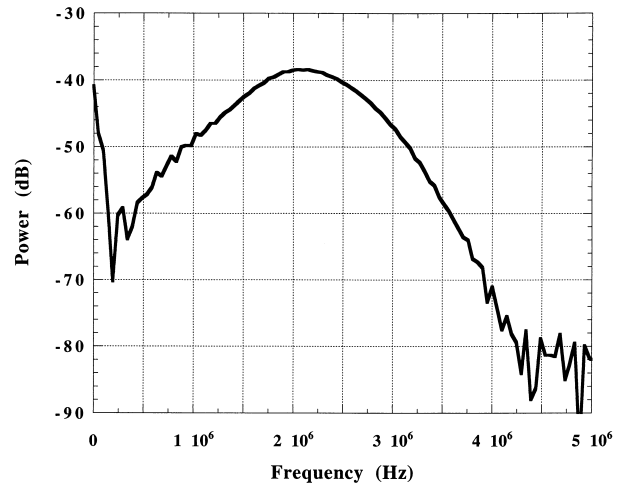

Figure 7. A typical reference spectrum illustrating the frequency response of the measurement system used in this study. The power spectrum was obtained by propagating an ultrasonic pulse from the transmitting transducer to the receiving transducer with no intervening specimen.

Bone Vol. 26, No. 6
June 2000:635–642

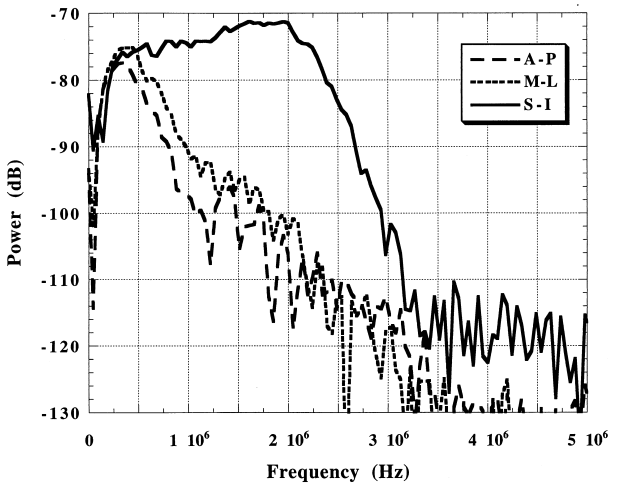

Figure 8. Power spectra obtained from ultrasonic pulses propagated along three different directions (anteroposterior, mediolateral, superoinferior) through a specimen of cancellous bone.

bone should demonstrate the same density dependence of BUA as specimens of less dense human cancellous bone.

AIB was analyzed by selecting a 4 μs portion of the backscattered signal from the sample using a rectangular window. The window was positioned to exclude the first 2 μs of the signal that was dominated by a large specular echo produced at the water-sample interface. Assuming a speed of sound of 2500 m/sec in cancellous bone, our analysis interrogated a region of bone approximately 5.0 mm thick, starting 2.5 mm behind the incident surface of the sample. **Figure 10** shows a typical backscattered signal, window location, and corresponding location in the sample.

One reason we chose to analyze backscatter using a relatively short-duration 4 μs window was to reduce the effects of attenuation on our backscatter measurements. As illustrated in Figure 10, attenuation produces an exponential decrease in the amplitude of the backscattered signal, leaving only the first few

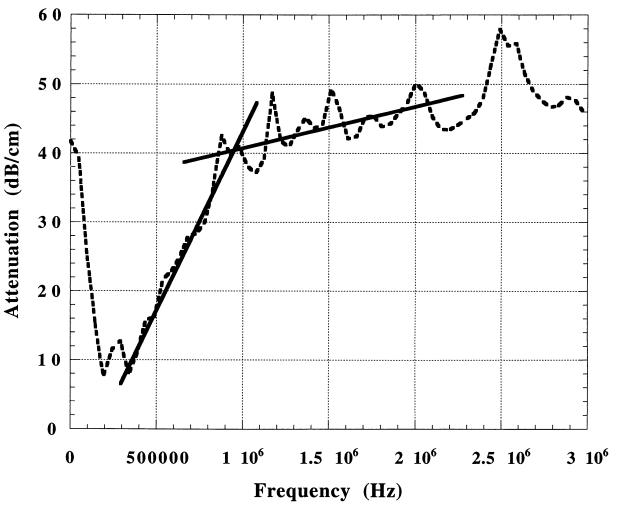

Figure 9. Frequency dependence of attenuation for a sample of cancellous bone. The lines superimposed on this graph illustrate the sudden change in slope of attenuation (i.e., BUA) near 1 MHz. This feature was noted for approximately half the samples investigated.

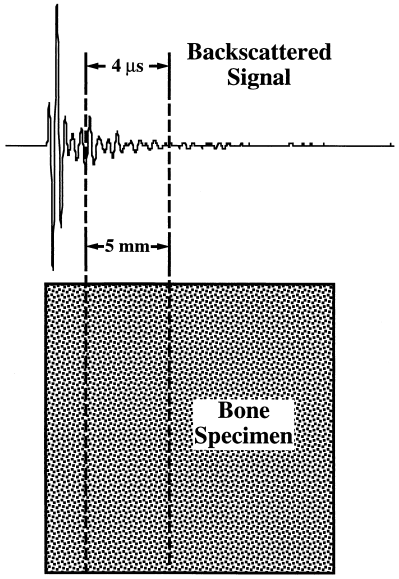

Figure 10. A typical ultrasonic signal backscattered from a specimen of cancellous bone. The 4 μs portion of the signal that was analyzed to determine apparent integrated backscatter (AIB) was selected to exclude the large specular echo occurring at the incident surface of the sample as shown.

microseconds that contribute significantly to the backscattered power. Portions of the signal arriving after the termination of the window are increasingly affected by attenuation because of the increased amount of intervening bone.

Our choice of window duration influenced our choice of bandwidth for the analysis of AIB. For our specific equipment and procedure, a 4 μs window yielded a frequency resolution of approximately 0.2 MHz. Over the bandwidth 1.0–3.0 MHz used for our analysis, each value of AIB therefore represented the backscattered power averaged over ten different frequencies spanning this bandwidth. We chose not to report results over much narrower bandwidths, such as those used for our analysis of BUA, because the number of values involved in this averaging process would decrease considerably, leading to increased variance.

It is of interest to compare our backscatter measurements to similar measurements performed on human cancellous bone by Wear and Garra.[24] Their method of acquiring data in vivo using an ultrasonic imaging system with a phased-array transducer was very different from the method employed in the present study. However, our measured parameter (AIB) and their measured parameter (relative ultrasonic backscatter) are similar in the sense that they both represent a measure of backscattered power uncompensated for the effects of attenuation. Wear and Garra observed that backscatter increased with BMD over a range of approximately 0.1–0.2 g/cm^3 (as measured using quantitative CT). We observed that backscatter decreased in bovine cancellous bone over a range of apparent densities of 0.3–0.9 g/cm^3. These results do not necessarily contradict each other because the ranges of densities investigated in each study may be substantially different. Over a sufficiently wide range of densities, one might expect backscatter to exhibit a similar density dependence as Serpe and Rho noted for BUA.[18] They showed that, at low densities, BUA increased with density and, at high densities, it decreased with density. To explain this behavior, Strelitzki et al. developed a theoretical model that assumed scattering to be the principal mechanism for ultrasonic attenuation in cancellous

bone.[21] They treated the inhomogeneous nature of cancellous bone as velocity fluctuations in a binary mixture (marrow fat and cortical matrix), and noted that the coefficient of scattering is proportional to these fluctuations. Their analysis showed that the mean velocity fluctuations of bone should increase with porosity, reach a maximum, and then decrease. Based on these considerations we hypothesize that the density dependence of AIB is not linear over a wide range of densities, and that it may increase over a range of densities and then decrease after reaching a maximum at some intermediate density.

Additional insight about the ultrasonic scattering properties of bone may be gained by further considering the physical interaction of acoustic waves with inhomogeneous media. Scattering occurs when the wave encounters inhomogeneities that possess a different acoustic impedance than the surrounding medium. In the case of this particular study, the fundamental scattering entities are probably the individual trabeculae.[24] The directionality and intensity of the scattered acoustic field depend on the shape of the trabeculae and their size relative to the ultrasonic wavelength. For the range of velocities and frequencies reported in this study, the wavelengths in the specimens of cancellous bone ranged between approximately 0.7 and 7 mm. Microstructural features of cancellous bone, such as the diameters of individual trabeculae, are typically 0.5 mm or less,[16] thus a discussion of scattering phenomena can be reasonably limited to cases in which the ultrasonic wave is longer than, or approximately the same size as, the scatterer.

To obtain a limited understanding of the ultrasonic scattering behavior of cancellous bone, one can approximate a single trabecula as a rigid cylinder of radius a, and the incident ultrasonic wave as an acoustic plane wave of intensity I and (angular) frequency ω. As discussed by Morse and Ingard,[14] if the plane wave is incident perpendicular to the cylinder axis, then the scattered intensity, I_s, is given by the first-order approximation:

$$I_s \cong \frac{\pi \omega^3 a^4}{8c^3 r} I(1 - 2\cos\phi)^2 \qquad (4)$$

where c is the speed of sound in the embedding medium (water or marrow), r is the radial distance from the scatterer, and ϕ is the angle relative to the incident direction ($\phi = 180°$ for backscatter). This result is valid for the long wavelength limit ($\omega a \ll c$). In this limit, it is of interest to note that the scattered intensity is strongly frequency dependent, and distributed predominantly in the backward direction. As the frequency increases and the wavelength approaches the radius of the cylinder, the angular distribution of the scattered field becomes increasingly more complicated, and Equation 4 becomes increasingly less valid. However, in the long- and short-wavelength limits, the total power scattered by the cylinder per unit length, Π_s, may be described approximately by the relatively simple expressions:

$$\Pi_s \cong \frac{3\pi^2 a^4 \omega^3}{4c^3} I \qquad \omega a \ll c \qquad (5)$$

$$\Pi_s \cong 4aI \qquad \omega a \gg c \qquad (6)$$

Thus, over a sufficiently broad range of frequencies, the frequency dependence of the intensity of the scattered acoustic field can change considerably.

Based on these theoretical observations we hypothesize that the transition from the long-wavelength limit to the short-wavelength limit may affect the frequency dependence of attenuation. This assumes that scattering is an important mechanism of attenuation. This is consistent with the observations of the present study, because the frequency dependence of attenuation decreased in many specimens for frequencies of >1 MHz. However, it is important to emphasize that Equations 4–6 are only approximations. The trabeculae are not necessarily well modeled as rigid cylinders, and the ultrasonic wave is not always perpendicular to the cylinder axis. In addition, these equations assume that the ultrasonic wave interacts with a single scatterer. While it may be reasonable to assume that the intensity of the scattered field scales with the number of scatterers, the number density of scatterers may be sufficiently large in cancellous bone that more complicated effects, such as multiple scattering, occur.

Future studies will be required to address some of the limitations of the present study. The most significant limitation involves the fact that all measurements were performed in vitro using specimens of bovine cancellous bone with the marrow removed. Extrapolation of our results to an in vivo situation involving less dense human bone should be done carefully. For example, it is not clear how bone marrow and the presence of intervening tissue between the transducers and region of interest may affect AIB and BUA in the range of frequencies reported in this study. Measurements obtained from an intact tibia or other bone would be very useful. In addition, the higher density of bovine cancellous bone may affect ultrasonic scattering in a fundamentally different manner than human bone through mechanisms such as multiple scattering. Repeating this study on specimens of human cancellous bone would be valuable using a similar in vitro procedure.

Ultrasonic backscatter may represent a useful new approach for the clinical assessment of bone. Wear and Garra demonstrated the clinical feasibility of backscatter-based measurements by showing that ultrasonic backscatter correlates strongly with BMD. The present study describes how to perform similar ultrasonic measurements under in vitro conditions using a measurement system that is less costly than a commercial imaging system. In vitro measurements are important for understanding the interaction of high-frequency ultrasonic waves with cancellous bone. For example, properties such as mass density and trabecular orientation may be determined directly from the specimens rather than inferred indirectly from X-ray measurements and anatomic location. In vitro measurements may also facilitate direct control of certain properties of the specimens, such as mineral or collagen content, to determine how backscatter and other ultrasonic properties depend on these constituents of cancellous bone. Other effects, such as the presence of intervening cortical bone and soft tissue, may also be investigated systematically using in vitro techniques.

References

1. Bamber, J. C., Fry, M. J., Hill, C. R., and Dunn, F. Ultrasonic attenuation and backscattering by mammalian organs as a function of time after excision. Ultrasound Med Biol 3:15–20; 1977.
2. Burke, T. M., Madsen, E. L., and Zagzebski, J. A. A preliminary study on the angular distribution of scattered ultrasound from bovine liver and myocardium. Ultrason Imag 9:132–145; 1987.
3. Campbell, J. A. and Waag, R. C. Measurements of calf liver ultrasonic differential and total scattering cross sections. J Acoust Soc Am 75:603–611; 1984.
4. Chivers, R. C. and Hill, C. R. A spectral approach to ultrasonic scattering from human tissue: Methods, objectives and backscattering measurements. Phys Med Biol 20:799; 1975.
5. Fei, D. Y. and Shung, K. K. Ultrasonic backscatter from mammalian tissues. J Acoust Soc Am 78:871–876; 1985.
6. Gluer, C. C., Wu, C. Y., Jergas, M., Goldstein, S. A., and Genant, H. K. Three quantitative ultrasound parameters reflect bone structure. Calcif Tissue Int 55:46–52; 1994.
7. Han, S., Rho, J. Y., Medige, J., and Ziv, I. Ultrasound velocity and broadband

attenuation over a wide range of bone mineral density. Osteopor Int 6:291–296; 1996.
8. Hoffmeister, B. K., Wong, A. K., Verdonk, E. D., Wickline, S. A., and Miller, J. G. Comparison of the anisotropy of apparent integrated ultrasonic backscatter from fixed human tendon and fixed human myocardium. J Acoust Soc Am 97:1307–1313; 1995.
9. Hosokawa, A. and Otani, T. Acoustic anisotropy in bovine cancellous bone. J Acoust Soc Am 103:2718–2722; 1998.
10. Hoyt, R. M., Skorton, D. J., Collins, S. M., and Melton, H. E. Ultrasonic backscatter and collagen in normal ventricular myocardium. Circulation 69: 775–782; 1984.
11. Insana, M., Zagzebski, J., and Madsen, E. Acoustic backscattering from ultrasonically tissuelike media. Med Phys 9:848–855; 1982.
12. Langton, C. M., Palmer, S. B., and Porter, R. W. The measurement of broadband ultrasonic attenuation in cancellous bone. Eng Med 13:89–91; 1984.
13. Mottley, J. G. and Miller, J. G. Anisotropy of the ultrasonic backscatter of myocardial tissue: I. Theory and measurements in vitro. J Acoust Soc Am 83:755–761; 1988.
14. Morse, P. M. and Ingard, K. U. Theoretical Acoustics. Princeton, NJ: Princeton University; 1986; 400–418.
15. Nicholson, P. H. F., Haddaway, M. J., and Davie, M. W. J. The dependence of ultrasonic properties on orientation in human vertebral bone. Phys Med Biol 39:1013–1024; 1994.
16. Rho, J. Y., Kuhn-Spearing, L., and Zioupos, P. Mechanical properties and the hierarchical structure of bone. Med Eng Phys 20:92–102; 1998.
17. Rossman, P., Zagzebski, J., Mesina, C., Sorensen, J., and Mazess, R. Comparison of ultrasonic velocity and attenuation in the os calcis to photon absorptiometry measurements in the radius, femur, and lumbar spine. Clin Phys Physiol Meas 10:353–60; 1989.
18. Serpe, L. and Rho, J. Y. The nonlinear transition period of broadband ultrasound attenuation as bone density varies. J Biomech 29:963–966; 1996.
19. Slutsky, L. J. Ultrasonic chemical relaxation spectroscopy. In: Edmonds, P. D., Ed. Methods of Experimental Physics. Vol. 19. New York: Academic; 190.
20. Strelitzki, R. and Evans, J. A. On the measurement of the velocity of ultrasound in the os calcis using short pulses. Eur J Ultrasound 4:205–213; 1996.
21. Striletzki, R., Nicholson, P. H. F., and Paech, V. A model for ultrasonic scattering in cancellous bone based on fluctuations in a binary mixture. Physiol Meas 19:189–196; 1998.
22. Tavakoli, M. B. and Evans, J. A. The effect of bone structure on ultrasonic attenuation and velocity. Ultrasonics 30:389–395; 1992.
23. Turner, C. H. and Eich, M. Ultrasonic velocity as a predictor of strength in bovine cancellous bone. Calcif Tissue Int 49:116–119; 1991.
24. Wear, K. A. and Garra, B. S. Assessment of bone density using ultrasonic backscatter. Ultrasound Med Biol 24:689–695; 1998.
25. Wickline, S. A., Verdonk, E. D., and Miller, J. G. Three-dimensional characterization of human ventricular myofiber architecture by ultrasonic backscatter. J Clin Invest 88:438–446; 1991.

Date Received: May 12, 1999
Date Revised: February 8, 2000
Date Accepted: February 17, 2000